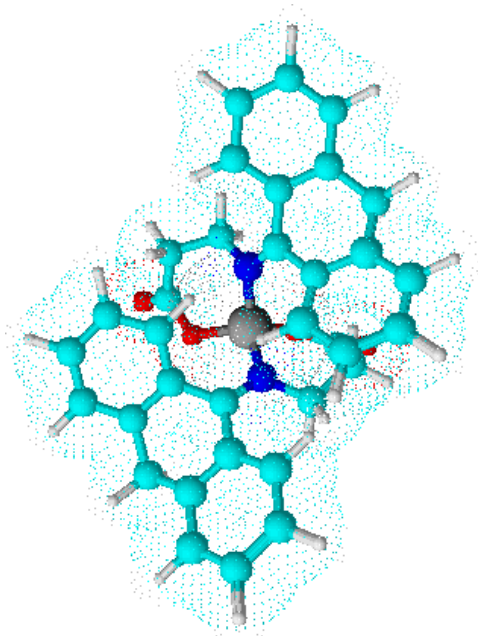


PART IV

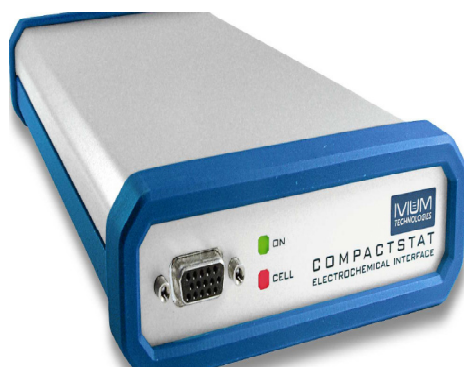
CYCLIC VOLTAMMETRIC STUDIES

Shaju. K. S. "Evaluation of metal evaluation binding capacity of azomethine class of compounds, electrochemical investigations on corrosion and their biological studies " Thesis. Department of Chemistry, St. Thomas College Thrissur, University of Calicut, 2014



PART IV

CYCLIC VOLTAMMETRIC STUDIES



CHAPTER 1

INTRODUCTION AND REVIEW

Cyclic voltammetry¹ (CV) “has become an important and widely used electro analytical technique in many areas of chemistry, particularly in organic and metal-organic systems. It is rarely used for quantitative determinations, but it is widely used for the study of redox processes, for understanding reaction intermediates and for obtaining stability of reaction products. This technique is based on varying the applied potential at a working electrode in both forward and reverse directions (at a particular scan rate) while monitoring the current. For example, the initial scan could be in the negative direction to the switching potential. At that point the scan would be reversed and run in the positive direction. Depending on the analysis, one full cycle, a partial cycle, or a series of cycles can be performed”.

Cyclic voltammetry is carried out in quiescent solution to ensure diffusion control. When the potential of the working electrode is more positive than that of a redox couple present in the solution, the corresponding species may be oxidized (i.e. electrons going from the solution to the electrode) and produce an anodic current. Similarly, on the return scan, as the working electrode potential becomes more negative than the reduction potential of a redox couple, reduction (i.e. electrons flowing away from the electrode) may occur to cause a cathodic current.

Usually the sweep is reversed at a specific switching potential, hence the name cyclic voltammetry. Since the sweep rate is constant and the initial and switching potentials are known, one can easily convert time to potential, and the usual protocol is to record current vs applied potential.

Cyclic voltammetric studies on Schiff bases and metal complexes – A review

Literature review shows that there are research articles on the electrochemical behaviour of novel Schiff bases²⁻⁶, complexes and organic compounds⁷⁻¹¹. Some of the important reviews are listed and discussed below.

“Cyclic voltammetric studies were used to investigate the interaction behaviour of the metal ions such as Cu(II) and Mn(II) with L-leucine by Habib et. al¹². The interaction studies have been carried out in variation of metal ion concentration, leucine concentration, pH and scan rate. The results indicated that Cu(II)/Cu(I) and Mn(II)/Mn(I) redox couple were reversible but Cu(I)/Cu(0) and Mn(II)/Mn(I) were quasi-reversible.

New Schiff base chelates of Cu(II), Co(II), Ni(II) and Zn(II) derived from benzil-2,4-dinitrophenylhydrazone with aniline have been synthesised. IR, ¹H NMR, ¹³C NMR, UV-Vis, CV and EPR spectral studies have been carried out by Raman¹³ and co-workers to suggest tentative structures for the complexes. The Cu(II) complex showed a well-defined redox process corresponding to the formation of the Cu(II)/Cu(I) couple. The CV of Zn(II) complex indicating quasi-reversible one electron process”.

Schiff base ligand was provided by Zare and Ataeinia¹⁴ “by means of 2,3-diaminopyridine and salicylaldehyde in absolute ethanol solvent with reflux method. The complexes of transition metals Fe, Cr and Co with the ligand were determined by using FT-IR, cyclic voltammetry (CV) and UV-Vis spectroscopy. The information obtained from cyclic voltammograms of the complexes showed that the electrochemical behaviour of the synthesized combinations indicates the reversible state of the complexes”.

“A series of complexes of Co(II), Ni(II), Cu(II), Mn(II) and Fe(III) have been synthesized by Kulkarni et. al¹⁵ with Schiff base derived from isatin monohydrazone and fluvastatin. The redox properties of the complexes were extensively investigated by electrochemical method using cyclic voltammetry (CV). The Co(II) and Cu(II) complexes exhibited quasi-reversible single electron transfer process where as Mn(II) and Fe(III) complexes showed two redox peaks of quasi-reversible one electron transfer process.

The electrochemical behaviour of three newly synthesized Schiff base Co(II)-complex with N₂SO donor group was investigated by Ershad et. al¹⁶. In different non-aqueous media such as acetonitrile (AN) and %50w/w CH₂Cl₂-DMSO mixture as aprotic solvents at the surface of solid electrodes (Pt, Au and GC) using tetra butyl ammonium perchlorate as supporting electrolytes, electrochemical behaviour studied by cyclic voltammetry. It has been found that, these compounds exhibit one or two quasireversible oxidation peaks and the charge transfer coefficients and the diffusion coefficients for these compounds in various solvents were obtained. The effect of scan rate and dielectric constant of solvents on the redox behavior of compounds were evaluated.

Salicylaldehyde, 2-hydroxyacetophenone and 3,5-dichloro salicylaldehyde were reacted with 1,2-diaminoethane to gave three symmetrical Schiff bases. With Ru(III) ions, these ligands lead to three complexes. The cyclic voltammetry in acetonitrile showed irreversible waves for all three ligands. These studies were carried out” by Ourari et. al¹⁷.

“Metal complexes of Schiff base (L) ligand, prepared by Pearl and Reji¹⁸ via condensation of 4- chlorobenzaldehyde and 4-aminoantipyrine.

Metal complexes were reported and characterized based on elemental analyses, IR, electronic spectra, magnetic moment, molar conductance and cyclic voltammetry (CV). The cyclic voltammogram of the Co(II) complex showed a well defined redox process corresponding to the formation of the quasi-reversible Co(II)/Co(I) couple. The redox property of Ni(II) complex displayed an irreversible cathodic peak corresponding to the reduction of Ni(II)/Ni(I).

A new tetradentate bis-benzimidazole based ligand, N-octyl-N,N'-bis-(2-methyl- benzimidazolyl)-benzene-1, 3-dicarboxamide(O-GBBA) has been synthesized and utilized to prepare iron (III) complexes by Sharma and Prasad¹⁹. Cyclic voltammetric measurements of the complexes displayed quasi reversible redox wave due to the Iron (III)/ Iron (II) redox process.

Tridentate Schiff base ligands were prepared by the condensation reaction of anthranilic acid with salicylaldehyde, furfural, thiophen-2-carboxaldehyde and pyridine-2-carboxaldehyde in ethanol” by Saghatforoush et. al²⁰. The electrochemical properties of four “Schiff base complexes of Co(II) have been investigated in the presence of tetra butyl ammonium perchlorate as supporting electrolyte and by using a glassy carbon (GC) electrode. It has been found that all the cobalt complexes showed Co(II) oxidation process irreversibility. Cyclic voltammetry studies indicated that these processes were diffusion-controlled reactions.

The electrochemical reduction of copper(II) complexes with salen Schiff base ligands derived from ethylenediamine or (R,R) or (S,S)-1,2-diphenylethylenediamine and 5-methoxy, 5-bromo and 5-nitrosalicylaldehyde have been studied by Zolezzi et. al²¹ using cyclic voltammetry in the potential

range +1 to -2.3 V in dimethyl sulfoxide (DMSO) as a solvent. The resulting voltammograms consist of a single quasi-reversible one-electron transfer attributable to the couple [Cu(II)L]/[Cu(I)L].

Cyclic voltammetry was used by Villamena and co-workers²² “to study the redox behaviour of complexes of the bidentate N-tert-butyl- α -(2-pyridyl)nitron (2-PyBN) and the monodentate nitron 2,5,5-trimethyl-1-pyrroline-N-oxide (M₃PO) with metal hexafluoroacetylacetonates M(hfac)₂ in CH₂Cl₂.

The complexation of new mixed thia-aza-oxa macrocycle viz., 2,12-dithio-5,9,14,18-tetraoxo-7,16-dithia-1,3,4,10,11,13-hexaazacyclooctadecane containing thiosemicarbazone unit with a series of transition metals Co(II), Ni(II) and Cu(II) has been investigated” by Chandra et. al²³. The redox behaviour was studied by cyclic voltammetry and explained that metal-centered reduction processes found in all complexes. The complexes of copper showed both oxidation and reduction processes.

“The interaction of the two newly synthesized transition-metal complexes, ML(2) (M=Co, Cu, L=1,8-dihydroxy ethyl-1,3,8,10,13-hexaazacyclotetradecane) with calf thymus DNA was probed by cyclic voltammetry (CV) and differential pulse voltammetry (DPV) by Lu et. al²⁴.

The binding specificity of the polymer to the template (Cu²⁺-2, 2'-dipyridyl complex) was investigated by Zeng et. al²⁵ using cyclic voltammetric scanning using the carbon paste electrode modified by polymer particles in phosphate buffer solution. The results demonstrated that cyclic voltammetry was an efficient approach to explore interactions between template and imprinted polymers”.

“The electrocatalytic reduction of sevoflurane has been carried out by Najafi et. al²⁶ at a platinum electrode using cyclic voltammetry. The results showed that, in a mixture with oxygen, cobalt(III) Schiff base complex (CoLOAc) and sevoflurane possess an irreversible peak at about -1.77 V versus Ag/AgCl (std) electrode.

Three copper(II) complexes derived from bulky ortho-hydroxy Schiff base ligands were synthesized” by Fernández et. al²⁷. Cyclic voltammetry studies performed for the complexes, indicate a dependence of the cathodic potentials upon conformational and electronic effects.

“The electrochemical behavior of some sulphha drug-Schiff bases at a mercury electrode was examined by Ghoneim and co-workers²⁸ in the Britton-Robinson universal buffer of various pH values (2.5–11.7) containing 20% v/v) of ethanol using DC-polarography, cyclic voltammetry and controlled-potential electrolysis. The DC-polarograms and cyclic voltammograms of the examined compounds exhibited a single, 2-electron, irreversible, diffusion-controlled cathodic step within the entire pH range which was attributed to the reduction of the azomethine group $-\text{CH}=\text{N}-$ to $-\text{CH}_2-\text{NH}-$.

The reaction of the Schiff base, 2-deoxy-2-(2-hydroxybenzaldimino)-D-glucopyranose with nickel acetate gave the bidentate, mononuclear Ni(II) complex that was characterized by Costamagna et. al²⁹ using cyclic voltammetry.

In the study by Çakır et. al³⁰, a novel Schiff base of cysteine and saccharin was synthesized and characterized by UV-Vis, FT-IR, ¹H NMR and elemental analysis. The voltammetric behaviour of Schiff base was investigated on the static mercury drop electrode (SMDE) using square-

wave voltammetry (SWV) and cyclic voltammetry (CV). The first reversible cathodic peak was due to reduction of the mercury thiolate, produced by the thiol group of Schiff base which adsorbs at Hg electrode surface, to metallic mercury and free thiol. The second reduction peak might be assigned to the reduction of azomethine centre ($>C=N-$) in the Schiff base and the last peak possibly related to the catalytic hydrogen reduction”.

Metal complexes were synthesized by Neelakantan³¹ et. al with “Schiff bases derived from o-phthalaldehyde (opa) and amino acids viz., glycine (GLY) L-alanine (ALA), L-phenylalanine (PAL). The cyclic voltammograms of the Cu(II)/Mn(II)/VO(II) complexes were investigated in DMSO solution and exhibited metal centered electro activity in the potential range -1.5 to +1.5V. The electrochemical data obtained for Cu(II) complexes explains the change of structural arrangement of the ligand around Cu(II) ion.

The Schiff base complexes of thiophene-2-carboxaldehyde and L-histidine with Co(II), Ni(II), Cu(II) and Zn(II) were synthesized and characterized by Muthuselvan³² et. al using elemental analysis, molar conductance, IR, UV-Vis, magnetic moment, thermal analyses and cyclic voltammetric investigations”.

Scope of present investigation

Amino acids derived metal complexes and amino acid Schiff bases are important class of organic compounds that are helpful in understanding biological functions of macromolecules. Transition metal complexes of azomethine compounds have been extensively investigated as catalysts for a number of organic redox reactions. Cyclic voltammetry has been a useful tool to investigate the interaction behaviour of metal ions with azomethine

compounds and to study the electrochemical behaviour of azomethine compounds. The extensive literature study clearly showed that there are only few reports on cyclic voltammetric studies of polynuclear Schiff base of amino acids and their metal complexes. There is no notable work has been reported on the CV studies of azomethine compounds derived from anthracene-9(10H)-one -amino acids. In the present work, the electrochemical behaviour of six potential Schiff base ligands A9Y3APA, A9Y5GPA, A9Y3IMPA, A9Y3INPA, A9Y3PPA, A9Y3MPA and few metal complexes were studied using cyclic voltammetry.

CHAPTER 2

MATERIALS AND METHODS

The materials used for the cyclic voltammetric studies, interpretation strategies of voltammogram, instrument and methods are discussed in this chapter.

Materials

Cyclic voltammetric measurements were carried out on the synthesized Schiff bases A9Y3APA, A9Y5GPA, A9Y3IMPA, A9Y3INPA, A9Y3PPA, A9Y3MPA and some copper (II) and zinc(II) complexes. Measurements were made on the deaerated (N_2 bubbling for 15 min.) solutions in DMSO (10^{-3} M) and 0.25 ml of citrate buffer containing 2 ml of 0.1 M tetra butyl ammonium tetra fluoro borate (TBATFB) as the supporting electrolyte.

Interpretations of voltammogram

In cyclic voltammetry, “the electrode potential ramps linearly versus time. This ramping is known as the experiment's scan rate (V/s). The potential is measured between the reference electrode and the working electrode and the current is measured between the working electrode and the counter electrode. This data is then plotted as current (i) vs. potential (E). The forward scan produces a current peak for any analytes that can be reduced (or oxidized, depending on the initial scan direction) through the range of the potential scanned. The current will increase as the potential reaches the reduction potential of the analyte, but then falls off as the concentration of the analyte is depleted close to the electrode surface. For the reversible redox couple systems, when the applied potential is reversed, it will reach the potential that will reoxidize the product formed by the first reduction and produce a current

of reverse polarity from the forward scan. This oxidation peak will usually have a similar shape to the reduction peak. As a result, information about the redox potential and electrochemical reaction rates of the compounds are obtained. For instance if the electronic transfer at the surface is fast and the current is limited by the diffusion of species to the electrode surface, then the current peak will be proportional to the square root of the scan rate.

Since the electrochemical properties are responsive with respect to the chemical environment and electron density, the respective peak and couples formed during CV conditions are mainly depending upon the electron transformations". Previous studies by researchers³⁴⁻³⁶ "indicate that during the electron transfer step, the probability of coupled chemical reactions, intramolecular reductive coupling, self protonation reactions etc were taken into account while interpreting the voltammogram".

"The important parameters of cyclic voltammetry are the magnitude of the peak currents, i_{pa} and i_{pc} , and the potentials at which peaks occur, E_{pa} and E_{pc} . Reversible peaks have a distinct absolute potential difference between the reduction peak (E_{pc}) and oxidation peak (E_{pa}). If the electron transfer process is fast compared with other processes (such as diffusion), the reaction is said to be electrochemically reversible, and the peak separation is

$$\Delta E_p = |E_{pa} - E_{pc}| = 2.303 \frac{RT}{nF}$$

Thus, for a reversible redox reaction at 25°C with n electrons ΔE_p should be $0.0592/n$ V or about 60 mV for one electron. In an ideal system $|E_{pc}-E_{pa}|$ would be 59 mV for a 1 electron process and 30 mV for a 2 electron" process³³. In practice this value is "difficult to attain because of such factors as cell

resistance. Irreversibility due to a slow electron transfer rate results in greater ΔE_p value than 70 mV for a one-electron reaction.

The formal reduction potential (E^0) for a reversible couple is given by

$$E^0 = \frac{E_{pc} + E_{pa}}{2}$$

The figure 4.1 shows a typical voltammogram, starting the scan from positive to negative direction.

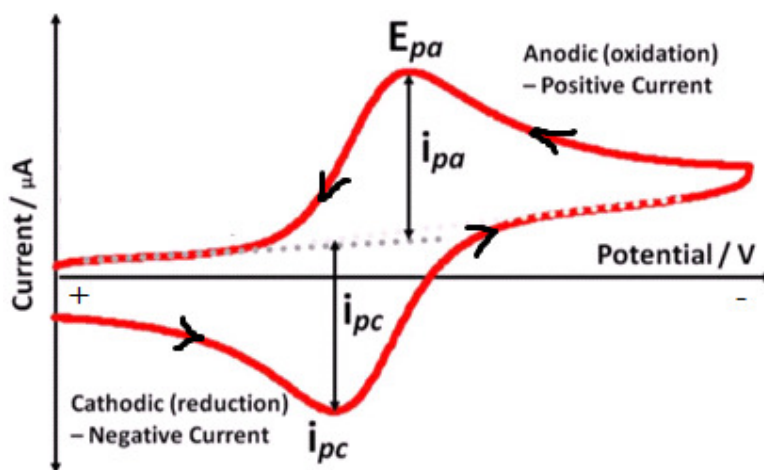


Fig. 4.1: Cyclic Voltammogram with scan initiated in negative direction

For a reversible reaction, the concentration is related to peak current by the Randles–Sevcik expression³⁷ (at 25°C):

$$i_p = 2.686 \times 10^5 n^{3/2} A C D^{1/2} \nu^{1/2}$$

where i_p is the peak current (in amperes), n is the number of electrons passed per molecule of analyte oxidized or reduced, A is the electrode area (in cm^2), C is the concentration of analyte in bulk solution (in mol/l) and D is the diffusion coefficient of analyte (in cm^2/sec) and ν is the potential sweep rate (in volts/sec). The peak current will increase linearly as a function of the square root of the scan rate for reversible electron transfer. Plots of i_p versus $\nu^{1/2}$ are useful in the characterization of electrochemical reversible redox

systems. Deviations from linearity are indicative either of complications in the kinetics of the observed electron transfer, or the result of the chemical changes which occur as a result of the electron transfer.

In addition, the ratio of the currents passed at reduction (i_{pc}) and end oxidation (i_{pa}) is near unity ($i_{pa}/i_{pc}=1$) for reversible peaks. When such reversible peaks are observed, thermodynamic information in the form of half cell potential $E^0_{1/2}$ can be determined. When waves are semi-reversible (quasi-reversible) i_{pa}/i_{pc} is less than or greater than 1 and then it can be possible to determine even more information especially kinetic processes. When waves are non-reversible it is impossible to derive what will be their thermodynamic $E^0_{1/2}$. The nature of multicycle voltammogram can be used for the analysis of adsorption³⁸ behaviour of the molecules on the glassy carbon electrode”.

Instrument and method

The cyclic voltammetry studies were carried out in an Ivium compactstat-e electrochemical system with three electrode assemblies which were connected to a personal computer assisted with software “Ivium soft”. The three electrode system consisted of glassy carbon (working), platinum wire (counter) and Ag/AgCl (reference) electrodes.

The figure 4.2 shows the experimental set up for the cyclic voltammetric studies. Cyclic voltammetric experiments were performed at room temperature in the wide potential range of +2 to -2 V, at sweep rates (v) 40 - 100 mV s⁻¹ for finding out the active region where the peaks are observed and selected particular potential region for further analysis.

The potential is first varied linearly in one direction and the scan direction is reversed and the potential is returned to its original value. The

excitation cycle is often repeated several times. The initial potential is designated as E_{start} and the potential at which reversal takes place is called switching potential (E_{sw}). Depending upon the composition of the sample, the direction of the initial scan may be either negative or positive. A scan in the direction of more negative potentials is termed as forward scan, while one in the opposite direction is titled as reverse scan.

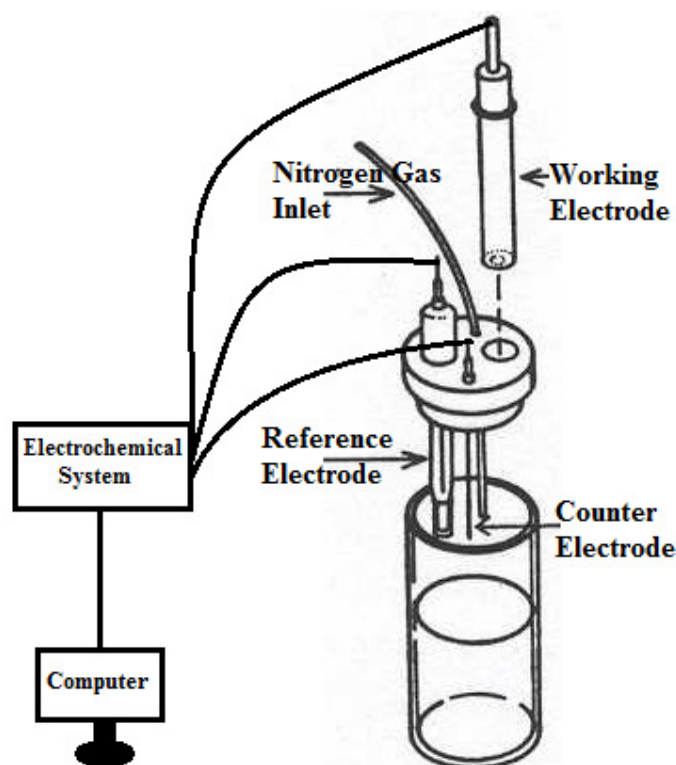


Fig. 4.2: Schematic diagram for experimental set up for Cyclic Voltammetric studies

After the voltammetric analysis, the significant peaks in the voltammogram were detected by automatic or advanced peak finding tool in the 'Ivium soft' software. Example for a typical cyclic voltammogram generated by Ivium soft together with labelled peaks is depicted in the figure 4.3.

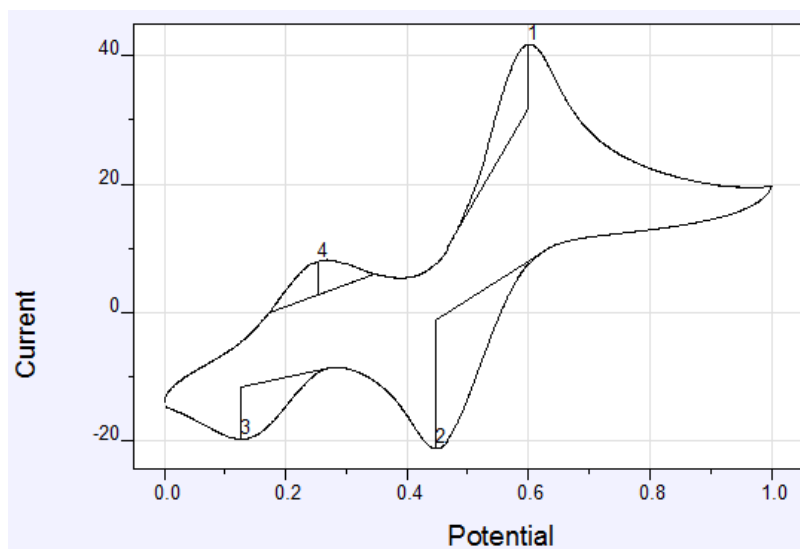


Fig. 4.3: Plot of typical Cyclic Voltammogram generated by Ivium soft

Interpreting complex cyclic voltammogram is often a challenge best met by the combination of chemical intuition with the study of model compounds, exactly in the same manner used by many spectroscopists to interpret optical, nmr and mass spectra.

CHAPTER 3

CYCLIC VOLTAMMETRIC STUDIES ON SCHIFF BASES AND COMPLEXES

A large number of Schiff bases and their metal complexes have been investigated for their interesting and important properties, for example, their ability to reversibly bind oxygen and complexing ability towards transition metals, furthermore complexes of Schiff bases showed promising applications in biological activity and biological modelling application. A plethora of references describing the Schiff bases and their metal complexes have appeared in the literature during the past few decades. However, little is known on the detailed electrochemical studies of such complexes. In view this, this chapter reports electrochemical behaviour of Schiff bases (A9Y3APA, A9Y5GPA, A9Y3IMPA, A9Y3INPA, A9Y3PPA, A9Y3MPA) derived by the condensation reaction of anthracene-9(10H)-one with various amino carboxylic acids and few of their metal complexes .

CV studies on the Schiff base A9Y3APA

The cyclic voltammogram of the Schiff base A9Y3APA was recorded at room temperature in the wide potential range of 2.0 V to -2.0 V at a scan rate of 0.04 - 0.1 V/s. The figures 4.4 and 4.5 show the cyclic voltammograms of A9Y3APA at a scan rate of 0.1V/s and 0.04 to 0.1 V/s respectively. Since the peaks were observed in the potential region between 0.0 V to -1.0 V, this scan range was sufficient for the analysis and represented in the figures. Three peaks were observed in the voltammogram of A9Y3APA which are labelled as A, B and C in the figure 4.4. During the forward scan, the two peaks A and B were appeared in the CV which was due to the two consecutive reductions

of the molecule. In the reverse scan, appearance of the peak C was due to the oxidation of the product resulting from the events accounting for peak B.

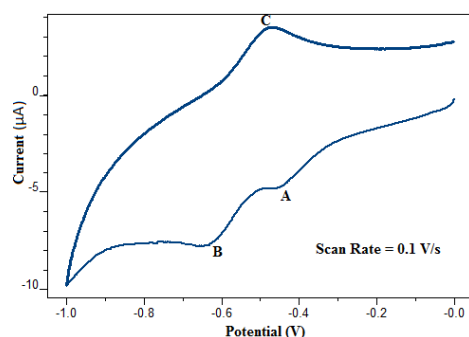


Fig. 4.4: Cyclic Voltammogram of A9Y3APA at a scan rate of 0.1 V/s

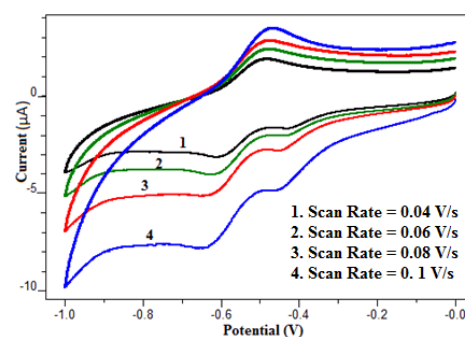


Fig. 4.5: Cyclic Voltammogram of A9Y3APA at scan rates 0.04 - 0.1 V/s

The E_{pc} value of peak A and peak B for the scan rate 0.1 V/s were -0.450 V and -0.637 V respectively while E_{pa} value of peak C was -0.469 V. The peak separation (ΔE_p) of the redox couple [peak B & peak C] was 0.168 V. The cathodic peak current, i_{pc} corresponds to peak A and peak B were 0.562 μA and 1.562 μA respectively and the anodic peak current, i_{pa} , for the peak C was 1.13 μA . Table 4.1 shows the complete cyclic voltammetric data of the Schiff base A9Y3APA.

Table 4.1. Cyclic Voltammetric data for Schiff base A9Y3APA

Scan Rate (V/s)	Redox Couple/ Peak	E_{pa} (V)	E_{pc} (V)	ΔE_p	i_{pa} (μA)	i_{pc} (μA)	i_{pa}/i_{pc}
0.04	B/C	-0.488	-0.611	0.123	0.928	1.072	0.9
	A	-	-0.426	-	-	0.259	-
0.06	B/C	-0.479	-0.626	0.147	0.940	1.18	0.8
	A	-	-0.432	-	-	0.289	-
0.08	B/C	-0.478	-0.626	0.148	0.973	1.290	0.8
	A	-	-0.448	-	-	0.379	-
0.10	B/C	-0.469	-0.637	0.168	1.13	1.562	0.7
	A	-	-0.450	-	-	0.562	-

The peak separation value shows that the redox couple involves one electron transfer. The ratio of the anodic to cathodic peak height is less than one which indicates the semi-reversible nature of the system. A probable mechanism for the electrochemical response of A9Y3APA can be explained as follows. At first, azomethine group present in the molecule undergo one electron reduction process which causes to appear a clear signal, A during the forward scan. As the potential become more negative, the complete reduction of azomethine moiety takes place, which is indicated by a peak B. The schematic representation of the mechanism is given in figure 4.6. During the reverse scan the appearance of peak C can be attributed to the oxidation of the completely reduced azomethine moiety present in the molecule.

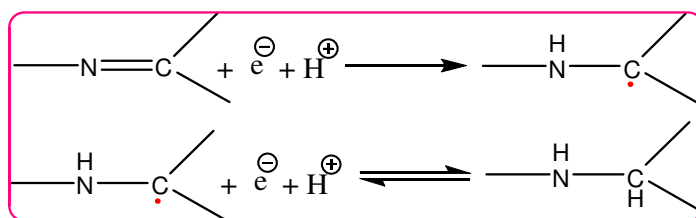


Fig. 4.6: Mechanism of redox process at azomethine moiety of A9Y3APA

Effect of scan rate and multiple scan on the voltammogram of A9Y3APA

ΔE_p value was found to increase with the scan rates, which give evidence for the quasi-reversible nature of the system. The intensity of both anodic and cathodic peaks was controlled by the Randles-Sevcik equation. The figure 4.7 depicts the plot of peak current, i_p against square root of scan rate $[v]^{1/2}$. From figure 4.7, it is clear that the peak current increases linearly with the square root of the scan rate which establishes that the electrode processes are diffusion controlled.

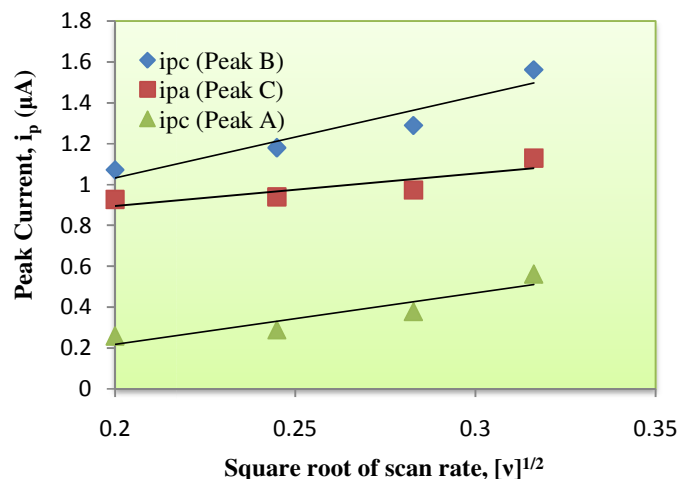


Fig. 4.7: Plot of peak current against square root of scan rate of A9Y3APA

The cyclic voltammogram of Schiff base with multiple scan cycles (number of cycles = 5) at a scan rate of 0.1 V/s is shown in the figure 4.8. It is evident from the figure that there is no appreciable change in the E_p and i_p values occurred during the multiple scan and it is confirmed that A9Y3APA molecules are not adsorbed on the electrode surface.

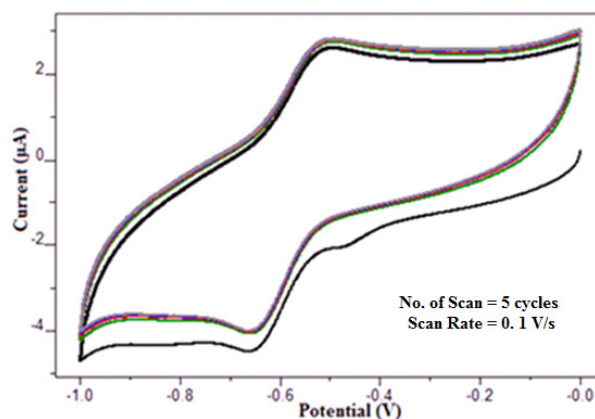


Fig. 4.8: Cyclic Voltammogram of Schiff base A9Y3APA with multiple scan cycles

CV studies on the Zn(II)-A9Y3APA complex

In the cyclic voltammetric curve (figure 4.9) for the electrochemical reduction of Zn(II)-A9Y3APA complex, a redox couple was appeared in the potential range 0 to -1.0 V at a scan rate of 0.1 V/s. On comparison, the cyclic

voltammograms of the ligand A9Y3APA and its Zn(II) complex, it can be seen that the peaks were shifted to more negative potential region in the complex. The reduction and oxidation peak was appeared at $E_{pc} = -0.833$ V and $E_{pa} = -0.573$ V respectively in the voltammogram of Zn(II)-A9Y3APA complex.

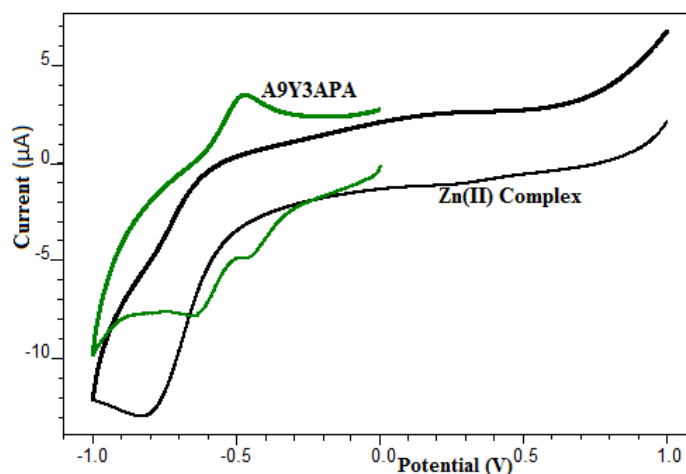


Fig. 4.9: Cyclic Voltammogram of A9Y3APA and Zn(II)-A9Y3APA complex at a scan rate of 0.1 V/s

The peak separation (ΔE_p) of the redox couple present in the CV of Zn(II)-A9Y3APA complex was 0.260 V. The corresponding cathodic peak current (i_{pc}) and anodic peak current (i_{pa}) were 3.636 μ A and 0.936 μ A respectively. Also the ratio of the anodic to cathodic peak height was less than one.

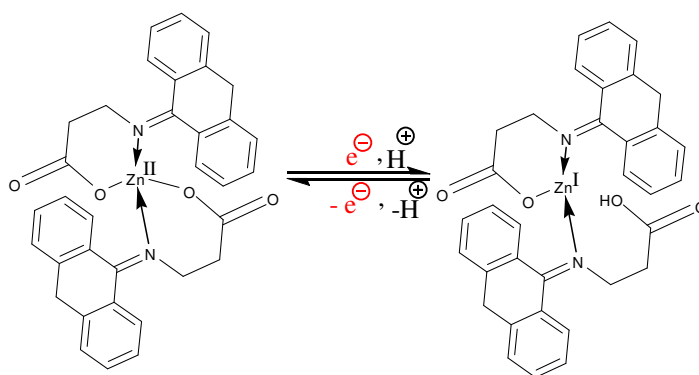


Fig. 4.10: Mechanism for the redox process of Zn(II)-A9Y3APA complex

The ΔE_p value and i_{pa} / i_{pc} value showed that the complex exhibit one electron quasi reversible transfer process for the redox couple Zn(II)/Zn(I). A probable mechanism which explains the redox behaviour of Zn (II)-A9Y3APA complex is depicted in the figure 4.10.

CV studies on the Schiff base A9Y5GPA

The electrochemical response of the Schiff base A9Y5GPA was studied by recording the cyclic voltammogram in the potential range +1.0 V to -1.0 V. The figure 4.11 shows the CV of A9Y5GPA at a scan rate of 0.1 V/s. On close observation of the figure, it can be seen that there are one cathodic peak represented by A and three anodic peaks represented by B, C and D. The E_p and i_p values of the various peaks are listed in the table 4.2. From the figure 4.11 and table 4.2, the electrochemical characteristic of A9Y5GPA can be interpreted as follows.

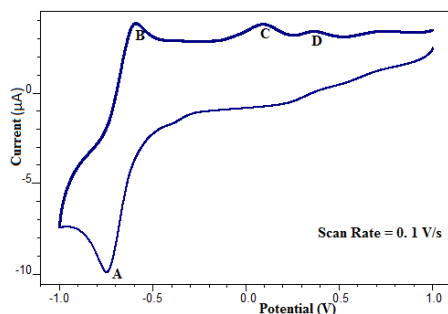


Fig. 4.11: Cyclic Voltammogram of A9Y5GPA at a scan rate of 0.1 V/s

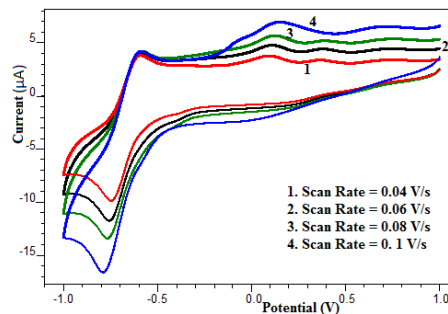


Fig. 4.12: Cyclic Voltammogram of A9Y5GPA at scan rates 0.04 - 0.1 V/s

The peak A appeared at -0.790 V can be considered due to the two electron reduction process of the azomethine moiety into saturated system. The involvement of two electrons was assumed, since the height of this cathodic peak was significantly higher than the other normal peaks. The two oxidation peaks observed at B and C can be attributed to the two successive

oxidation process of the reduced form of the Schiff base. Thus the original molecule regenerates at a higher oxidation potential of 0.390 V. The overall mechanism of the redox process is depicted in the figure 4.13. The third oxidation peak D appeared at 0.142 V in the voltammogram may be due to the involvement of arginine moiety.

Table. 4.2. Cyclic Voltammetric data for Schiff base A9Y5GPA

Scan Rate (V/s)	Redox Peak	E _{pa} (V)	E _{pc} (V)	i _{pa} (μA)	i _{pc} (μA)
0.04	A	-	-0.747	-	5.03
	B	-0.589		3.105	
	C	0.083	-	0.569	-
	D	0.362	-	0.246	-
0.06	A	-	-0.758	-	5.382
	B	-0.588		3.30	
	C	0.110	-	0.609	-
	D	0.374	-	0.285	-
0.08	A	-	-0.766	-	5.75
	B	-0.585		4.172	
	C	0.120	-	0.871	-
	D	0.388	-	0.197	-
0.10	A	-	-0.790	-	7.08
	B	-0.589	-	4.66	-
	C	0.142	-	0.990	-
	D	0.390	-	0.394	-

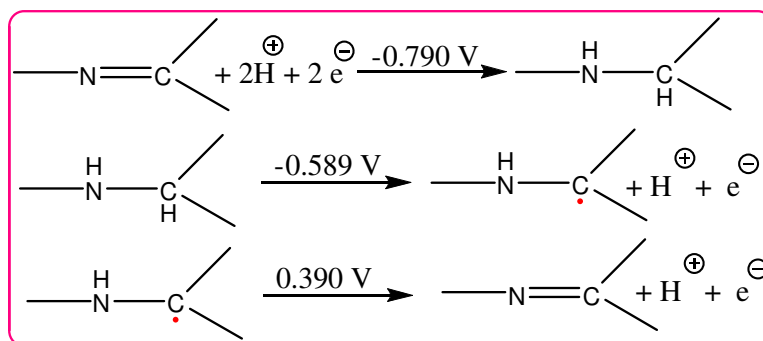


Fig. 4.13: Mechanism of redox process at azomethine moiety of A9Y5GPA

Effect of scan rate and multiple scan on the voltammogram of A9Y5GPA

Figure 4.12 shows the cyclic voltammogram of A9Y5GPA at different scan rate. As the scan rate increases, the E_{pc} values are shifted to more negative potentials. For the peaks B, C and D, no counter cathodic peak was observed in the voltammogram. Similarly counter anodic peak was absent for the reduction process designated by 'A' and it may be concluded that the reduction and oxidation process occurred in the potential range -1 to +1 V for the Schiff base A9Y5GPA were irreversible in nature.

The variation of i_p values with the square root of scan rate is depicted in the figure 4.14. The current-scan responses (i_p versus $v^{1/2}$, Randles-Sevcik representation) are straight lines that exhibit slight deviations from linearity. The deviations from linearity suggested a change from a diffusion-controlled process to a mixed control process³⁹.

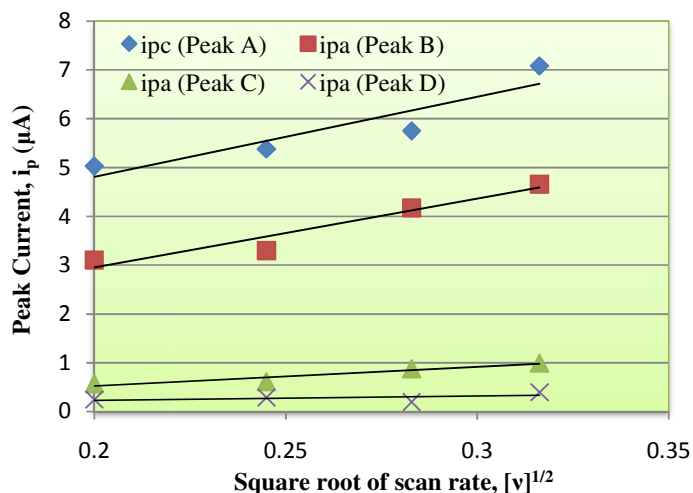


Fig. 4.14: Plot of peak current against square root of scan rate of A9Y5GPA

Figure 4.15 shows CV recorded at a scan rate of 0.1 V/s with 5 scan cycles. Since all the peaks were appeared in the same position in all the cycles, suggesting that there is no adsorption of the compound on the glassy carbon electrode surface.

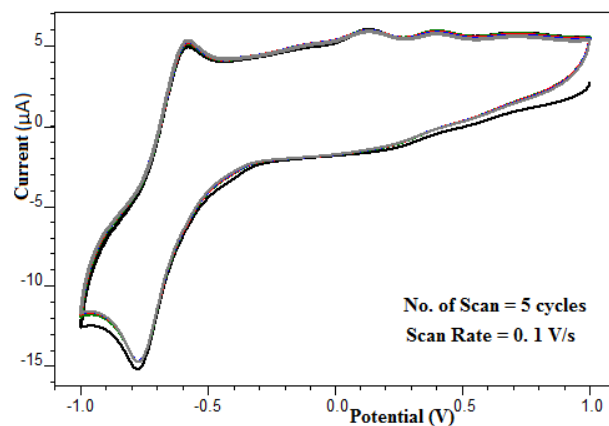


Fig. 4.15: Cyclic Voltammogram of Schiff base A9Y5GPA with multiple scan cycles

CV studies on the Cu(II)-A9Y5GPA complex

Figure 4.16 and 4.17 show the cyclic voltammogram of Cu(II) complex at a scan rate of 0.1 V/s and 0.04-0.1 V/s respectively. The table 4.3 exhibits the CV data of Cu(II) complex at different scan rates.

Table. 4.3. Cyclic Voltammetric data for Cu(II) - A9Y5GPA complex

Scan Rate (V/s)	E_{pa} (V)	E_{pc} (V)	ΔE_p	i_{pa} (μ A)	i_{pc} (μ A)	i_{pa}/i_{pc}
0.04	-0.507	-0.671	0.164	0.608	2.687	0.2
0.06	-0.511	-0.685	0.174	0.675	3.382	0.2
0.08	-0.526	-0.693	0.167	0.771	3.838	0.2
0.1	-0.528	-0.712	0.184	0.783	4.605	0.2

The cyclic voltammogram of Cu(II) complex (+1.0 V to -1.0V) at a scan rate of 0.1 V/s shows a quasi-reversible peak in the negative region, characteristic of the Cu(II) \rightarrow Cu(I) couple at $E_{pc} = -0.712$, with associated anodic peak at $E_{pa} = -0.528$ for Cu(I) \rightarrow Cu(II). On comparing the voltammogram of A9Y5GPA and its Cu(II) complex (Figure 4.16), it is evident that the oxidation peaks appeared in the voltammogram of Schiff base (peaks C and D) was totally disappeared on complexation.

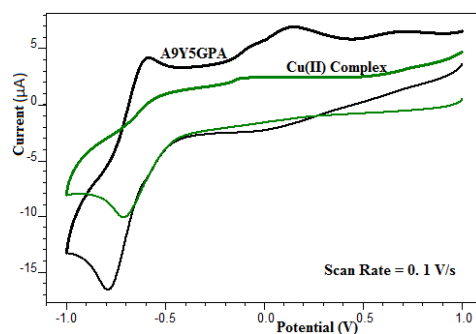


Fig. 4.16: Cyclic Voltammogram of A9Y5GPA and Cu(II) complex at a scan rate of 0.1 V/s

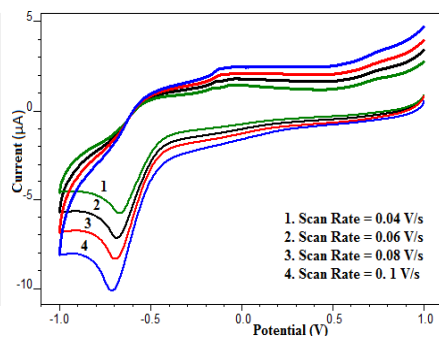


Fig. 4.17: Cyclic Voltammogram of Cu(II)-A9Y5GPA complex at scan rates 0.04 - 0.1 V/s

Effect of scan rate and multiple scan on the voltammogram of Cu(II) complex

It is apparent from table 4.3 that the ratio of anodic to cathodic peak height was less than one, however, the peak current density varies linearly with the square root of scan rate as shown in figure 4.18, which establishes the diffusion controlled nature of the electrode process. The peak separation value also increases with the scan rate, giving further evidence for the quasi-reversible Cu(II)/Cu(I) couple.

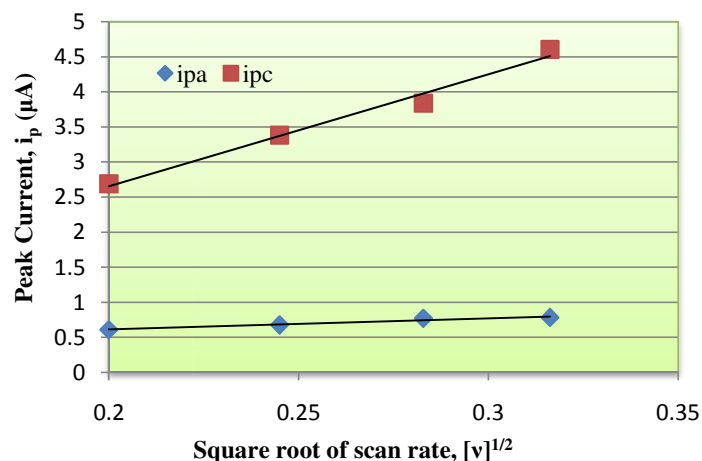


Fig. 4.18: Plot of peak current against square root of scan rate of Cu(II)-A9Y5GPA complex

At a scan rate of 0.1 V/s repetitive scans were carried out and the voltammogram are presented in the figure 4.19. The peaks were observed at the

same positions in each cycle and can suggest that the complex was not adsorbed on the electrode surface.

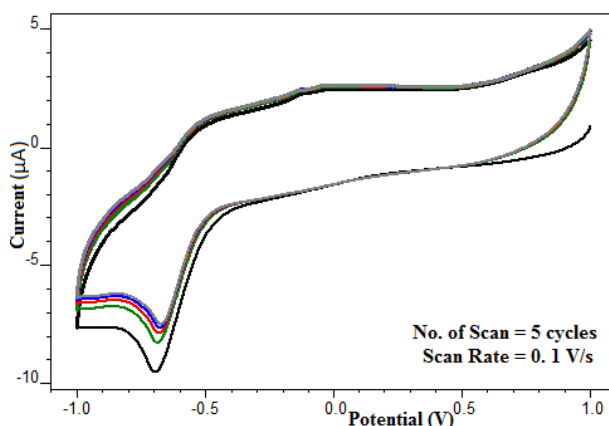


Fig. 4.19: Cyclic Voltammogram of Cu(II)-A9Y5GPA complex with multiple scan cycles

The cyclic voltammogram of the Zn(II) and Co(II) complexes didn't show any characteristic peak potential indicating that a strong complex was formed between A9Y5GPA and these metal ions.

CV studies on the Schiff base A9Y3IMPA

The cyclic voltammetric experiments were performed on the Schiff base A9Y3IMPA in the potential range +1 to -1 V at various sweep rates and the voltammograms are given in figures 4.20 and 4.21.

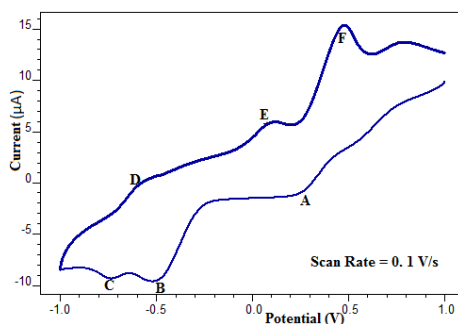


Fig. 4.20: Cyclic Voltammogram of A9Y3IMPA at a scan rate of 0.1 V/s

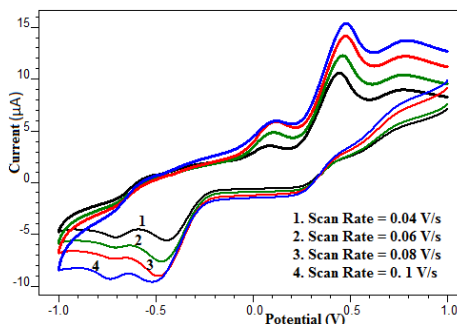


Fig. 4.21: Cyclic Voltammogram of A9Y3IMPA at scan rates 0.04 - 0.1 V/s

The voltammogram of A9Y3IMPA showed three redox couples in the scanned potential region. The voltammetric parameters of various redox couples are provided in table 4.4. Figure 4.20 shows the voltammogram of

Schiff base at the scan rate 0.1 V/s. At this scan rate, the ΔE_p values of the redox couple are 0.155, 0.986 and 0.161, which suggest that electrochemical process involve one electron transfer and the system behave in a quasi reversible manner. From the analysis of the figure 4.20, the mechanism of the redox behaviour can be described as follows.

Table. 4.4. Cyclic voltammetric data for Schiff base A9Y3IMPA

Scan Rate (V/s)	Redox Couple/ Peak	E_{pa} (V)	E_{pc} (V)	ΔE_p	i_{pa} (μA)	i_{pc} (μA)	i_{pa}/i_{pc}
0.04	A/E	0.071	0.268	0.197	0.668	0.966	0.7
	B/F	0.445	-0.447	0.892	1.772	2.048	0.9
	C/D	-0.585	-0.706	0.121	0.475	0.203	2.3
0.06	A/E	0.090	0.252	0.162	1.020	1.306	0.8
	B/F	0.461	-0.470	0.931	3.126	2.549	1.2
	C/D	-0.587	-0.707	0.120	0.503	0.334	1.5
0.08	A/E	0.097	0.267	0.170	1.267	1.356	0.9
	B/F	0.477	-0.485	0.962	4.577	3.629	1.3
	C/D	-0.572	-0.720	0.148	0.551	0.606	0.9
0.10	A/E	0.094	0.249	0.155	1.545	1.706	0.9
	B/F	0.478	-0.508	0.986	5.568	4.297	1.3
	C/D	-0.585	-0.746	0.161	0.874	0.705	1.2

During the forward scan, the cathodic peak observed at 0.249 V can be assigned to the reduction of imidazole moiety of the Schiff base A9Y3IMPA. The counter oxidation peak of this signal was appeared in the reverse scan at 0.094 V. The prominent cathodic peaks B and C emerged in the negative potential regions can be attributed to the two step reduction stages of the azomethine linkage of the molecule as represented in the figure 4.22. These reduction peaks were associated with two oxidation peaks, which appeared at

0.478 and -0.585 V respectively. Thus two significant redox couples B/F and C/D were originated in the voltammogram of A9Y3IMPA.

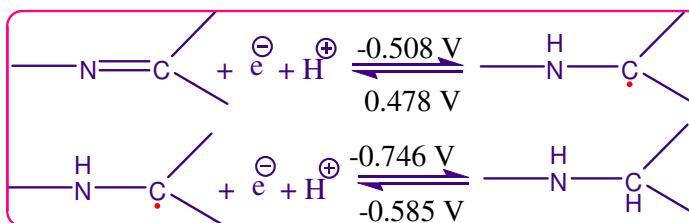


Fig. 4.22: Mechanism of redox process at azomethine moiety of A9Y3IMPA

Effect of scan rate and multiple scan on the voltammogram of A9Y3IMPA

Figure 4.21 shows the voltammogram of A9Y3IMPA at different scan rate in the potential region +1 V to -1 V. It can be seen from the figure that, as the scan rate increases the i_p values also increases. The plots of peak current against square root of the scan rate are depicted in the figures 4.23, 4.24 and 4.25 for various redox couples A/E, B/F and C/D respectively. The figures show a linear relationship between current and scan rate. The straight lines obtained for the redox couple A/E and B/F suggest that the electrode process are diffusion controlled. In the case of redox couple C/D, the current - scan rate relation deviate from linearity indicate that a change from a diffusion-controlled process to a mixed controll process (kinetic and diffusion) occurred at high scan rates.

The ratio of the anodic peak height to cathodic peak height (i_{pa}/i_{pc}) values were observed to be less than or greater than one which establishes that all redox process are quasi-reversible in nature.

Though being larger than the theoretical value for an electrochemically reversible one-electron process, ΔE_p data suggest that the reduction of the Schiff base under study should correspond to one-electron charge transfer. The

electrochemical properties of the Schiff bases are highly sensitive to the electron density and the azomethine moiety. So it is difficult to assign the correct redox couples present in the compound with respect to its structure.

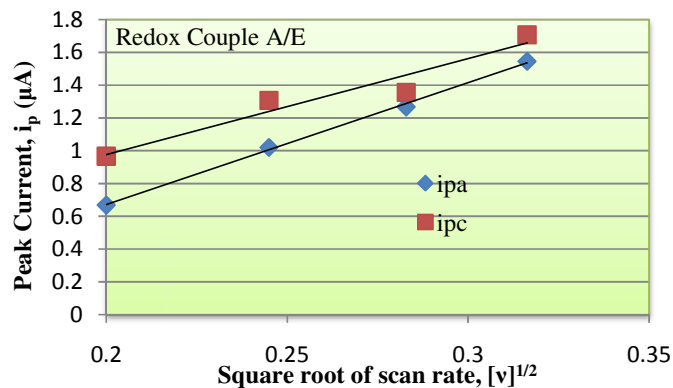


Fig.4.23: Plot of peak current against square root of scan rate for the redox couple A/E of A9Y3IMPA

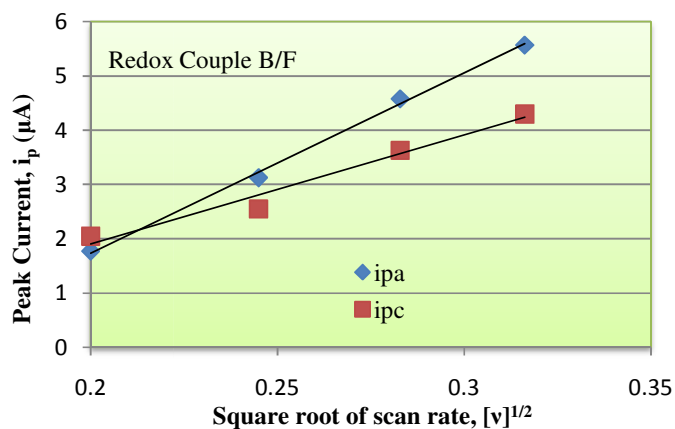


Fig.4.24: Plot of peak current against square root of scan rate for the redox couple B/F of A9Y3IMPA

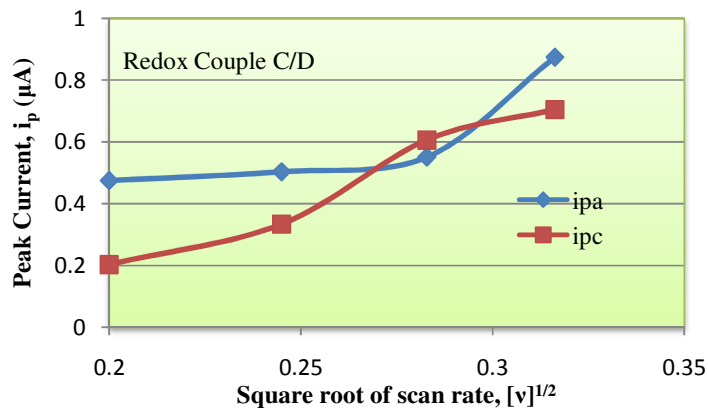


Fig. 4.25: Plot of peak current against square root of scan rate for the redox couple C/D of A9Y3IMPA

The effect of multiple scan on electrode process at scan rate 0.1V/s was also studied and represented in the figure 4.26. From the figure it is evident that no change in the peak positions during five cycles of scanning occurred and it is suggested that repetitive scan do not affect the electrode process.

The cyclic voltammetry of Co(II), Cu(II) and Zn(II) complexes of the Schiff base A9Y3IMPA were performed and no characteristic peaks are observed. This observation suggests that the metal ions in +2 oxidation state stabilize the ligand during complexation.

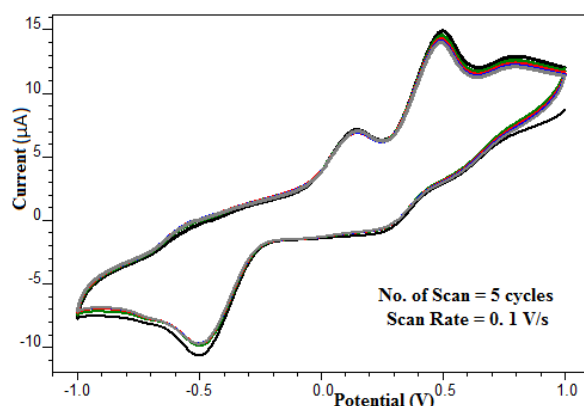


Fig. 4.26: Cyclic Voltammogram of Schiff base A9Y3IMPA with multiple scan cycles

CV studies on the Schiff base A9Y3INPA

The electrochemical behaviour of the Schiff base A9Y3INPA was studied by recording the cyclic voltammogram in the potential range +1.0 V to -1.0 V at different scan rate. Two cathodic peaks and two anodic peaks were observed in the cyclic voltammogram of A9Y3INPA. The cyclic voltammetric parameters of the Schiff base are presented in the table 4.5. The ΔE_p and i_{pa}/i_{pc} values indicates that electrode process involve one electron transfer and quasi reversible in nature. For the sake of discussion, the cyclic voltammogram (figure 4.27) at the scan rate of 0.01 V/s was chosen.

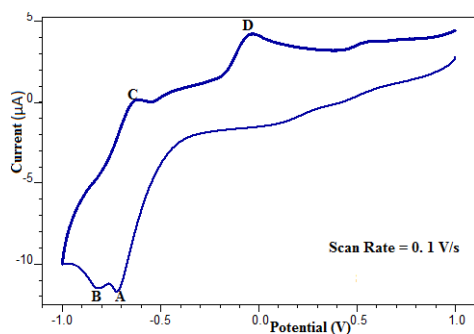


Fig. 4.27: Cyclic Voltammogram of A9Y3INPA at a scan rate of 0.1 V/s

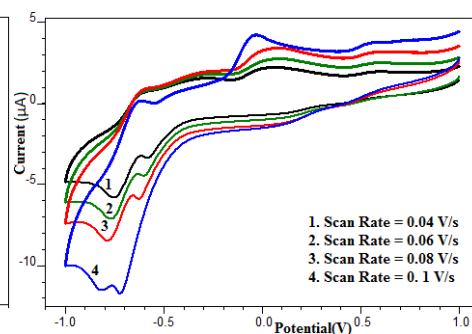


Fig. 4.28: Cyclic Voltammogram of A9Y3INPA at scan rates 0.04 - 0.1 V/s

Table 4.5. Cyclic Voltammetric data for Schiff base A9Y3INPA

Scan Rate (V/s)	Redox Couple/ Peak	E_{pa} (V)	E_{pc} (V)	ΔE_p	i_{pa} (μA)	i_{pc} (μA)	i_{pa}/i_{pc}
0.04	A	-	-0.583	-	-	0.322	-
	B/C	-0.623	-0.755	0.132	0.487	2.103	0.2
	D	0.054	-	-	0.652	-	-
0.06	A	-	-0.601	-	-	0.568	-
	B/C	-0.623	-0.769	0.146	0.635	2.145	0.3
	D	0.013	-	-	0.693	-	-
0.08	A	-	-0.626	-	-	0.748	-
	B/C	-0.623	-0.786	0.163	0.887	2.172	0.4
0.1	D	0.015	-	-	0.807	-	-
	A	-	-0.722	-	-	2.494	-
	B/C	-0.614	-0.829	0.215	1.456	2.252	0.6
0.1	D	-0.034	-	-	1.335	-	-

The overall electrochemical behaviour of A9Y3INPA in DMSO medium can be summarized as follows. The first cathodic peak displayed at -0.722 V is regarded to the reduction of the azomethine moiety of the Schiff base. As the potential become more negative, a second reduction peak was emerged at -0.829 which can be assigned for the second stage reduction of azomethine linkage. At this stage imine moiety of the molecule will be in a

completely reduced state as similar to the mechanism shown in figure 4.22. As the scan is reversed, the prominent oxidation peaks (C and D) and one broad oxidation peak were appeared in the voltammogram of A9Y3INPA. The signal displayed at -0.614 V and 0.559 V (broad) are due to the oxidation of the reduced form of the Schiff base in two stages as represented in the schematic diagram. Thus one can assume that at the peak potential 0.559 V, the original Schiff base molecule regenerate at the electrode surface. The oxidation peak appeared at -0.034 V may be due to the oxidation of the indole moiety of the Schiff base A9Y3INPA.

Effect of scan rate and multiple scan on the voltammogram of A9Y3INPA

As the scan rate is increased, the behaviour of Schiff base A9Y3INPA become more intricate, (figure 4.28). The peak separation ΔE_p and the current density i_p are also appreciably increased with the scan rate.

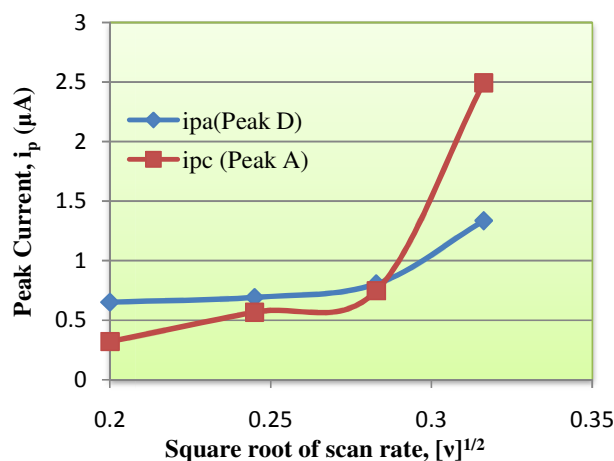


Fig. 4.29: Plot of peak current against square root of scan rate for the peaks A and D of A9Y3INPA

The variations of peak current with square root of scan rate are shown in the figure 4.29 and 4.30 respectively for the peaks A, D and redox couple B/C. The dependence of i_p with $v^{1/2}$ was found to be linear at low scan rates, but deviation from the linearity was noted with increasing sweep rate. This

behaviour suggest that the electrode process is diffusion controlled at low scan rates, whereas at high scan rates a transition to a mixed (kinetic and diffusion) controlled process take place.

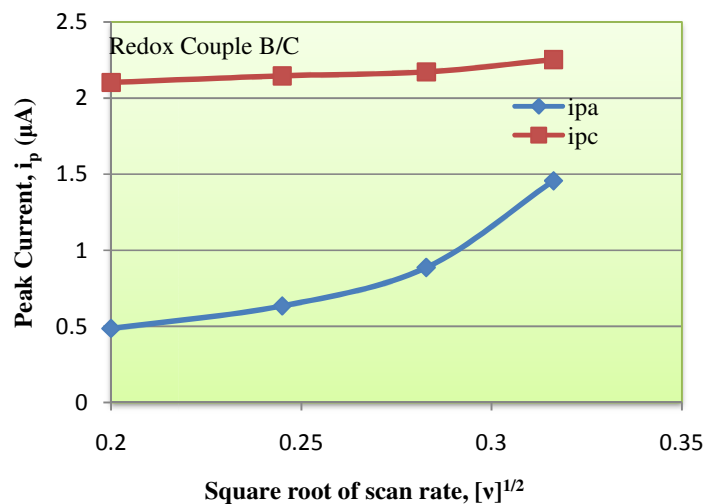


Fig. 4.30: Plot of peak current against square root of scan rate for the redox couple B/C of A9Y3INPA

The adsorption behaviour of the Schiff base on the electrode surface was determined by the multiple scanning at a scan rate of 0.1 V/s and the voltammograms obtained for the five cycles is presented in the figure 4.31. No appreciable change for the peak positions and the peak heights in the voltammogram suggest that the Schiff base is not absorbed on the glassy carbon electrode.

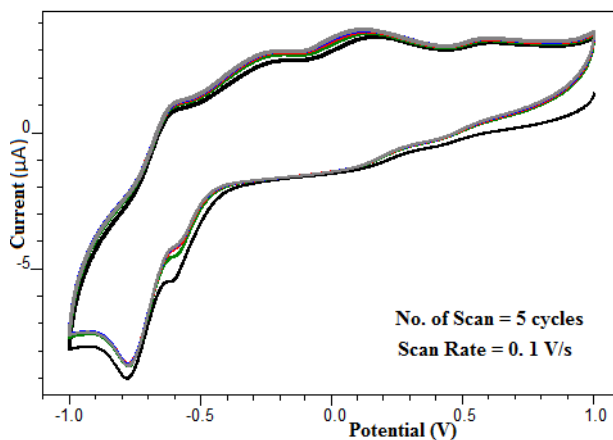


Fig. 4.31: Cyclic Voltammogram of Schiff base A9Y3INPA with multiple scan cycles

CV studies on the Schiff base A9Y3PPA

The redox behaviour of the Schiff base A9Y3PPA was investigated by recording the cyclic voltammogram in the potential range of +1.0 V to -1.0 V at different scan rate. The voltammograms recorded at a scan rate of 0.04 V/s and 0.04-0.1 V/s are depicted in figures 4.32 and 4.33 respectively. It is clear from the figure 4.32 that the voltammogram at 0.1 V/s has less number of peaks than voltammogram at lower scan rates.

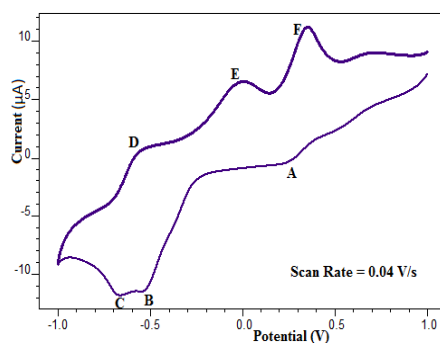


Fig. 4.32: Cyclic Voltammogram of A9Y3PPA at a scan rate of 0.04 V/s

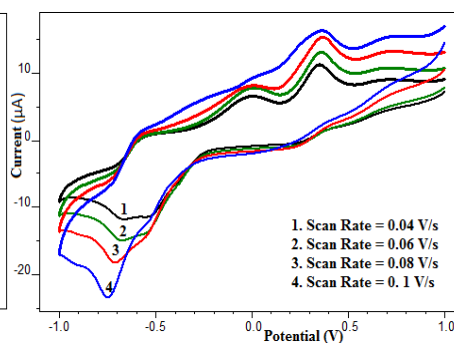


Fig. 4.33: Cyclic Voltammogram of A9Y3PPA at scan rates 0.04 - 0.1 V/s

The voltammogram at 0.04 V/s is characterized by three redox couple A/E, B/F and C/D with corresponding peak separations (ΔE_p) 0.238, 0.904 and 0.102 respectively. The respective anodic to cathodic current ratio i_{pa}/i_{pc} was 0.7, 1.8 and 1.2 respectively for these redox couples. Table 4.6 explores the complete CV parameters for the Schiff base A9Y3PPA at different scan rates. Since the ΔE_p values are higher than 0.059 V/s and i_{pa}/i_{pc} values are less than or greater than 1, it can be concluded that redox process involve one electron transfer and system behave in a quasi-reversible manner.

The mechanism of electrochemical behaviour of A9Y3PPA can be interpreted as follows. The peak displayed at 0.227 V may be due to the reduction of phenyl ring and the associated anodic peak displayed at -0.011 V

regarded as the oxidation of phenyl ring. The two reduction peaks appeared at -0.551 V and -0.672 V may be assigned to the two step reduction stages of the azomethine linkage of the molecule. These reduction processes are associated with two oxidation peaks which are appeared at 0.353 and -0.570 V. Thus two prominent redox couples B/F and C/D were emerged in the voltammogram of A9Y3PPA.

Table. 4.6. Cyclic Voltammetric data for Schiff base A9Y3PPA

Scan Rate (V/s)	Redox Couple/ Peak	E_{pa} (V)	E_{pc} (V)	ΔE_p	i_{pa} (μA)	i_{pc} (μA)	i_{pa}/i_{pc}
0.04	A/E	-0.011	0.227	0.238	2.104	3.118	0.7
	B/F	0.353	-0.551	0.904	4.342	2.35	1.8
	C/D	-0.570	-0.672	0.102	2.132	1.732	1.2
0.06	A/E	-0.007	0.223	0.23	2.371	3.354	0.7
	B/F	0.362	-0.545	0.907	4.646	2.751	1.7
	C/D	-0.570	-0.672	0.102	2.205	3.647	0.6
0.08	A/E	-0.033	0.238	0.271	2.676	3.732	0.7
	B/F	0.369	-0.541	0.91	5.237	3.01	1.7
	C/D	-0.585	-0.709	0.124	2.69	5.36	0.5
0.10	A	-	0.148	-	-	4.474	
	C/D	-0.596	-0.747	0.151	2.998	7.176	0.4
	F	0.347	-	-	5.828	-	

Effect of scan rate and multiple scan on the voltammogram of A9Y3PPA

The figure 4.33 indicates the presence of three cathodic peaks and three anodic peaks which were clearly appeared at the scan rates between 0.4 V/s to 0.8 V/s. In the case of voltammogram obtained for the scan rate of 0.1 V/s, there were only two anodic peaks and two cathodic peaks. The reduction and oxidation peak at B and E were totally absent at this scan rate. This may be due to the widening of the peaks. The peak currents were increased with the

scan rate, which is quite clear from table 4.6. The plots of i_p against square root of the scan rate are shown in the figure 4.34, 4.35 and 4.36 for the redox couple A/E, B/F, C/D respectively.

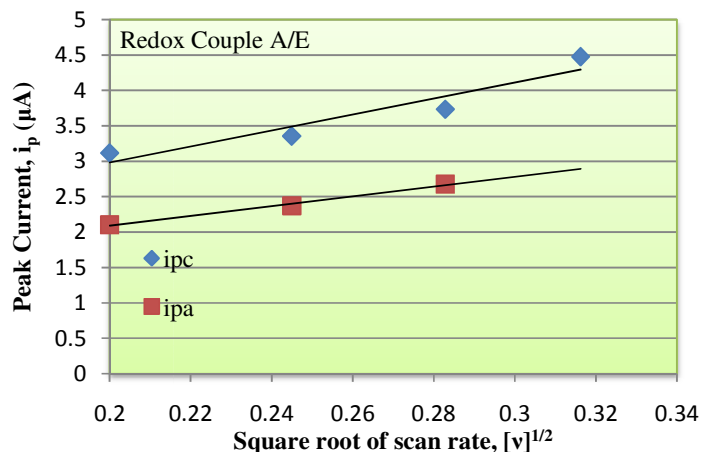


Fig. 4.34: Plot of peak current against square root of scan rate for the redox couple A/F of A9Y3PPA

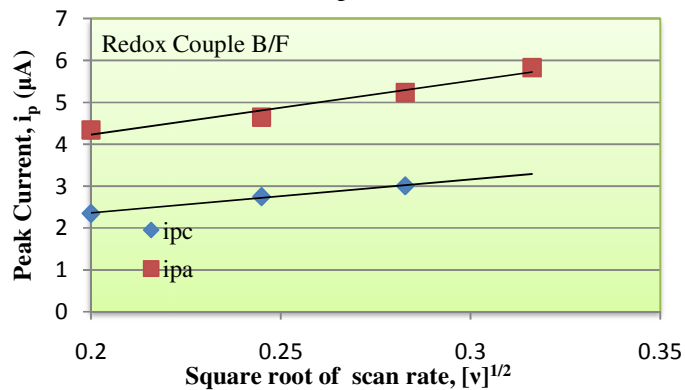


Fig. 4.35: Plot of peak current against square root of scan rate for the redox couple B/E of A9Y3PPA

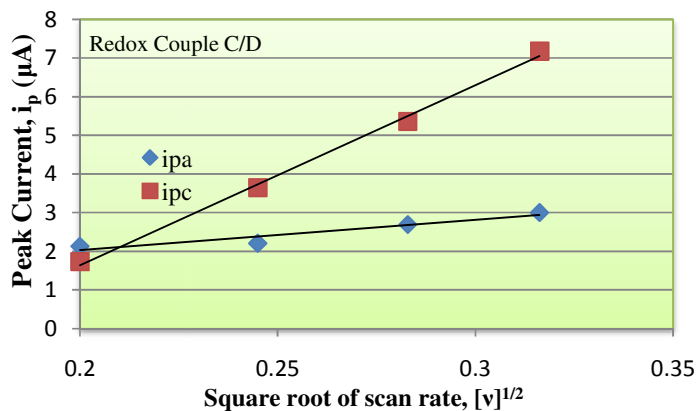


Fig. 4.36: Plot of peak current against square root of scan rate for the redox couple C/D of A9Y3PPA

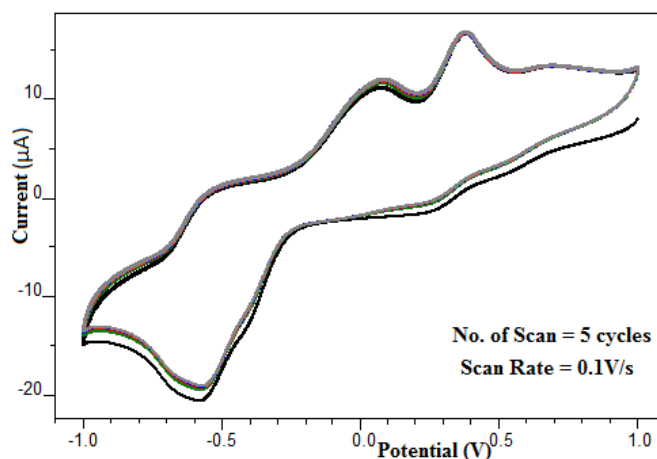


Fig. 4.37: Cyclic Voltammogram of Schiff base A9Y3PPA with multiple scan cycles

All figures show a linear relationship between the current and square root of scan rate and this linearity suggest that the electrode processes are diffusion controlled. The variation of ΔE_p with scan rate establishes that the redox process involve one electron transfer. In short, all the redox processes are quasi-reversible, diffusion controlled and involves the transfer of one electron.

It can also possible to determine by cyclic voltammetry whether the Schiff base A9Y3PPA adsorbed on the electrode surface or not. Figure 4.37 shows the consecutive votammogram of A9Y3PPA at a scan rate of 0.1 V/s. No significant change in the peak positions was noted in each cycle which clearly establishes that the Schiff base was not adsorbed on the working electrode appreciably.

CV studies on the Cu(II)-A9Y3PPA complex

In comparison to ligand, the CV (figure 4.38) of Cu(II)-A9Y3PPA complex exhibited only one redox couple between -0.739 to -0.095 V which can be attributed to the metal centred electrochemical process.

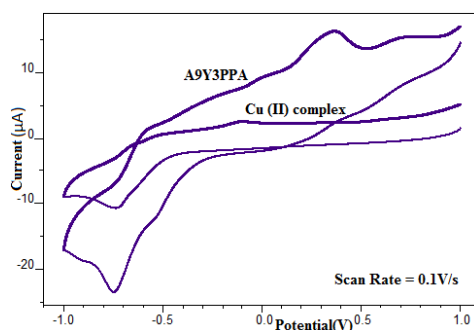


Fig. 4.38: Cyclic Voltammogram A9Y3PPA and Cu complex at a scan rate of 0.1 V/s

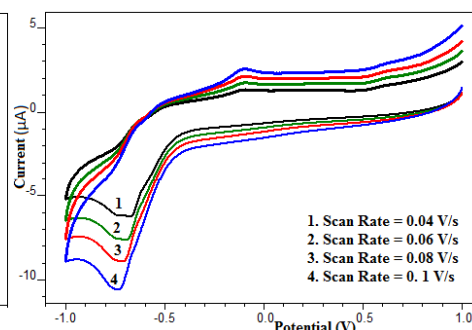


Fig. 4.39: Cyclic Voltammogram of Cu(II)-A9Y3PPA complex at scan rates 0.04 - 0.1 V/s

Table 4.7. Cyclic Voltammetric data for Cu(II)-A9Y3PPA complex

Scan Rate V/s	E_{pa} (V)	E_{pc} (V)	ΔE_p	i_{pa} (μA)	i_{pc} (μA)	i_{pa}/i_{pc}
0.04	-0.095	-0.706	0.611	0.920	1.759	0.5
0.06	-0.094	-0.721	0.627	1.254	2.223	0.6
0.08	-0.095	-0.706	0.611	1.610	2.663	0.6
0.1	-0.095	-0.739	0.644	2.060	2.922	0.7

The ΔE_p values were decreased slightly as the scan rate was lowered. Thus, analysis of cyclic voltammogram at different scan rates (figure 4.39) gives the evidence for quasi-reversible one electron reduction process. The redox couple present in the CV of copper complex may be expressed as:

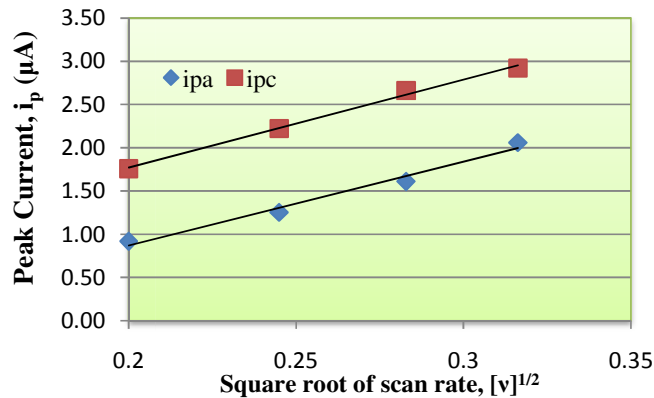
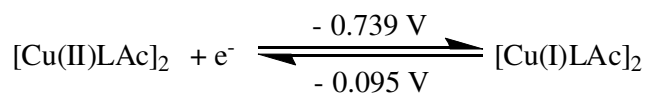


Fig. 4.40: Plot of peak current against square root of scan rate for Cu(II) -A9Y3PPA complex

The ratio of anodic to cathodic peak height was less than unity for all scan rates. However, the peak current was increased with the square root of the scan rate. The plot of i_p against $[v]^{1/2}$ for the redox couple (figure 4.40) shows a linear relationship which establishes that the electrode processes are diffusion controlled.

Effect of multiple scan on the voltammogram of Cu-A9Y3PPA complex

The adsorption behaviour of the Cu(II) complex was studied by recording the cyclic voltammogram (figure 4.41) at a scan rate of 0.1V/s with multiple scan (number of cycles=5). The peaks were observed almost in the same potential regions in each cycle, suggest that the complex molecules were not adsorbed on the electrode surface.

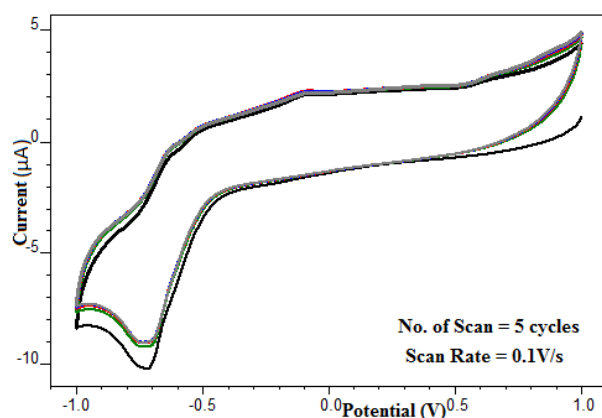


Fig. 4.41: Cyclic Voltammogram of A9Y3PPA-Cu(II) complex with multiple scan cycles

CV studies on the Schiff base A9Y3MPA

The cyclic voltammogram of the Schiff base A9Y3MPA in the potential range +1.0 to -1.0 V and at a scan rate 0.1 V/s is shown in the figure 4.42. The voltammogram exhibits only one irreversible oxidation peak at 0.325 V with a current 1.368 µA. CV of A9Y3MPA at different scan rate is depicted in the figure 4.43. From the figure it is evident that the peak values were changed with the scan rate. The peak potentials at scan rates 0.02, 0.04,

0.06 and 0.08 V/s were 0.183, 0.243, 0.288 and 0.318 respectively. The corresponding peak currents were 0.630, 0.757, 0.860 and 0.883 μA respectively for the different scan rates.

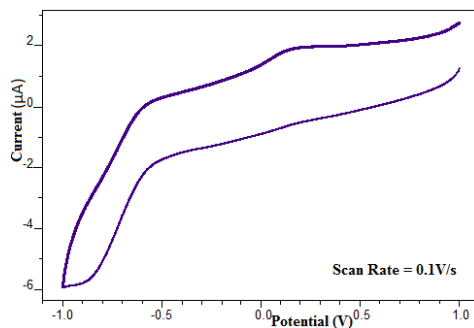


Fig. 4.42: Cyclic Voltammogram of A9Y3MPA at a scan rate of 0.1 V/s

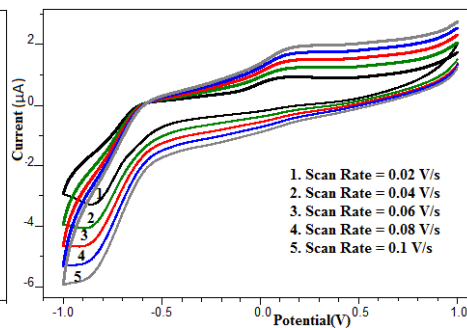


Fig. 4.43: Cyclic Voltammogram of A9Y3MPA at scan rates 0.02 - 0.1 V/s

In the CV of A9Y3MPA, the peaks corresponds to the reduction of azomethine linkage was not clearly observed may be due to the rapidness of the electrode process or masking of the peak current by the influence of polarisable sulphur moiety of the amino acid part. But a prominent peak observed at 0.325 V clearly represents the oxidation of the reduced molecular species which was very close to the oxidation potentials of the Schiff base molecules and the process can be represented as follows (figure 4.44).

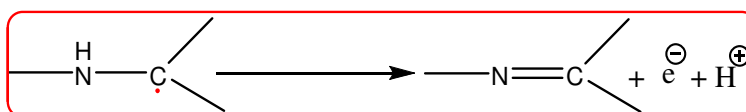


Fig. 4.44: Mechanism of oxidation process at azomethine moiety of A9Y3PPA

The consecutive scan cycles show that there is no appreciable peak shifts and therefore it can be concluded that the Schiff base was not adsorbed on the electrode surface.

CV studies on the Cu(II)-A9Y3MPA complex

The cyclic voltammogram of 10^{-3}M Cu(II) complex in DMSO is shown in the figure 4.45. The voltammogram at different scan rates are

presented in the figure 4.46. Analysis of each voltammogram at different scan rates gave cyclic voltammetric parameters which are presented in the table 4.8.

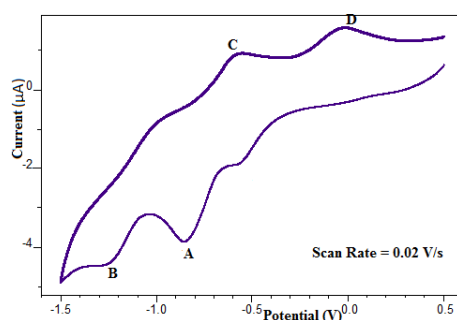


Fig. 4.45: Cyclic Voltammogram of Cu(II)-A9Y3MPA complex at a scan rate of 0.02 V/s

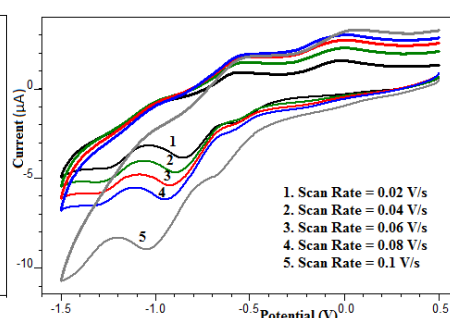


Fig. 4.46: Cyclic Voltammogram of Cu(II)-A9Y3MPA at scan rates 0.02-0.1 V/s

Table. 4.8. Cyclic Voltammetric data for Cu(II)-A9Y3MPA complex

Scan Rate V/S	Redox Couple Peak	E_{pa} (V)	E_{pc} (V)	ΔE_p	i_{pa} (μA)	i_{pc} (μA)	i_{pa}/i_{pc}
0.02	A/D	-0.014	-0.857	0.843	0.554	1.234	0.4
	B/C	-0.552	-1.252	0.7	0.374	0.375	1.0
0.04	A/D	0.004	-0.882	0.886	0.604	1.528	0.4
	B/C	-0.512	-1.247	0.735	0.660	0.425	1.6
0.06	A/D	0.002	-0.924	0.926	0.656	1.645	0.4
	B/C	-0.563	-1.289	0.726	0.928	0.484	1.9
0.8	A/D	0.005	-0.869	0.874	0.728	1.72	0.4
	B/C	-0.565	-1.296	0.731	1.161	0.557	2.1
0.1	B/C	-0.558	-1.036	0.478	1.271	0.680	1.9
	D	0.052	-	-	2.325	-	-

The voltammogram involve two cathodic peaks and two anodic peaks. At a scan rate of 0.02 V/s, the voltammogram shows quasi-reversible redox couple (A/D) with $\Delta E_p = 0.843$ V and $i_{pa}/i_{pc} = 0.4$ in the potential range 0.5 to -1.0 V. The second reox couple (B/C) with $\Delta E_p = 0.7$ V and $i_{pa}/i_{pc} = 1$ was also observed in the potential range -0.55 to -1.25 V. In the B/C redox couple, the ratio of anodic to cathodic peak height is equal to one which shows the

reversible nature of the system but the ΔE_p value was greater than 59 mV. Thus we can conclude that this redox process is pseudo-reversible at low scan rate. One electron transfer was assigned to all redox processes at different scan rates, since the ΔE_p values falls in the range 0.48 to 0.88. Since the i_{pa}/i_{pc} values of all redox couples except B/C are less than or greater than one, suggest that the nature of electrode process is quasi-reversible.

The variation of peak current with the square root scan rate is plotted in the figures 4.47 & 4.48 for the redox couple A/D & B/C respectively.

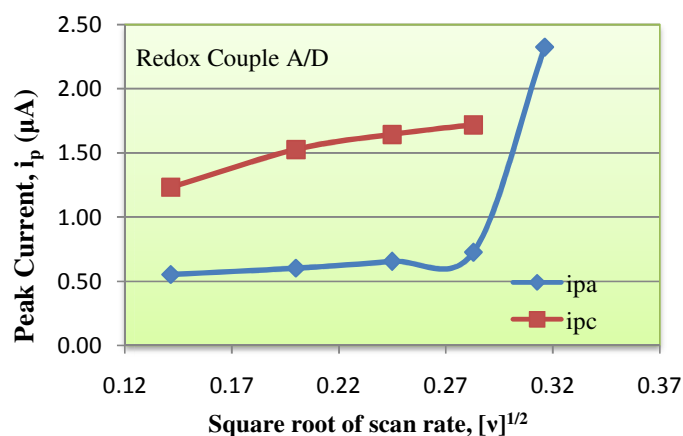


Fig. 4.47: Plot of peak current against square root of scan rate for the redox couple A/D of Cu(II)-A9Y3MPA

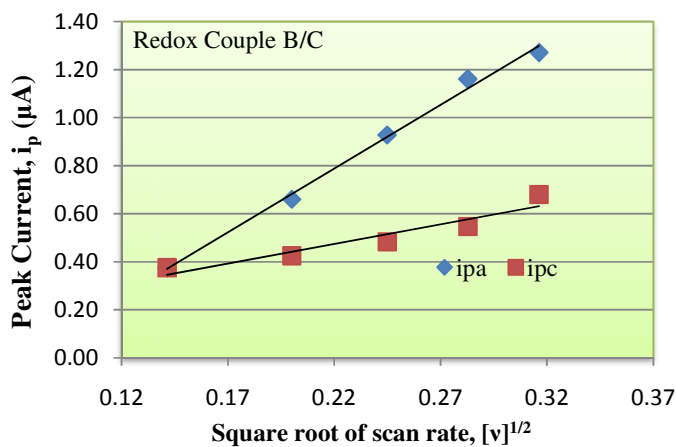


Fig. 4.48: Plot of peak current against square root of scan rate for the redox couple C/D of Cu(II)-A9Y3MPA

From the figures it is clear that the peak current increases with the square root of the scan rates which establishes the diffusion controlled electrode processes.

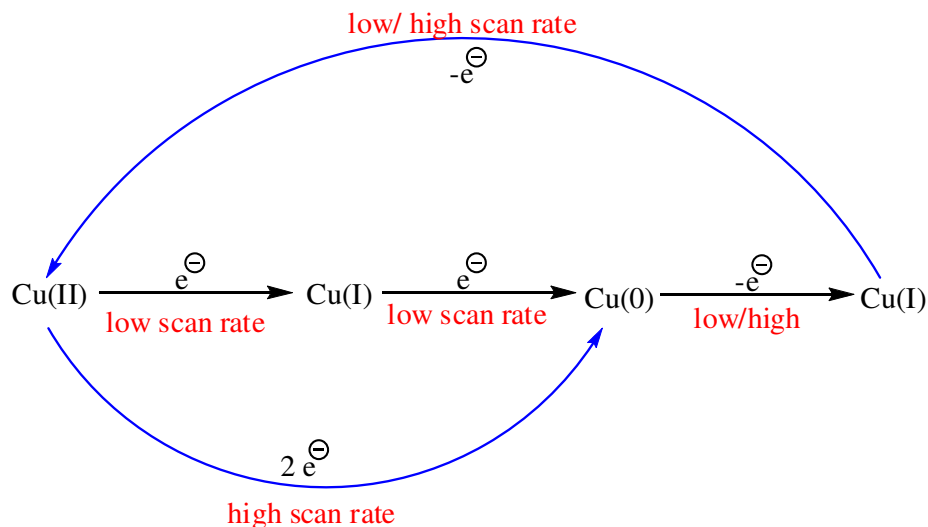


Fig. 4.49: Mechanism of redox process of Cu(II)-A9Y3MPA complex

Interestingly, in the voltammogram of Cu(II)- A9Y3MPA complex at a scan rate of 0.1 V/s , the cathodic peak A was disappeared. At high scan rates, the peaks were widened and the peak potential and the peak current were increased. The overall mechanism for the electrochemical behaviour of Cu(II)- A9Y3MPA system at low and high scan rates can be summarized as in figure 4.49.

Though electrode reactions are one electron process, the peak corresponds to the reduction of Cu(II) → Cu(I) was absent at high scan rate analysis. This can be attributed to the very high rate of the Cu(II) → Cu(I) conversion during the electrochemical reduction.

SUMMARY

Among the synthesized Schiff bases and their metal complexes, the six azomethine compounds, Zn(II)-A9Y3APA complex and Cu(II) complexes of A9Y5GPA, A9Y3PPA, A9Y3MPA were susceptible to the redox process under the conditions of cyclic voltammetry. The voltammogram of A9Y3APA exhibited one redox couple and one irreversible reduction peak. The Zn(II)-A9Y3APA complex showed only one redox peak which corresponds to Zn(II)/Zn(I) couple. The CV of A9Y5GPA displayed three irreversible oxidation peaks and one irreversible reduction peak. The voltammogram of Cu(II)-A9Y5GPA complex revealed only one redox couple and this may be due to Cu(II)/Cu(I) electrode process. CV studies on A9Y3IMPA exhibited three redox couples. Voltammogram of A9Y3INPA showed one redox couple, one irreversible reduction peak and one irreversible oxidation peak. The voltammogram of A9Y3PPA showed three redox couples and Cu(II)-A9Y3PPA complex showed only one redox couple corresponds to Cu(II)/Cu(I). The A9Y3MPA displayed only one irreversible oxidation peak and its Cu(II) complex showed two redox couples at scan rates 0.02 to 0.08 V/s. At scan rate of 0.1 V/s the Cu(II)-A9Y3MPA complex exhibited one redox couple and one irreversible oxidation peak.

The peaks were emerged in the cyclic voltammogram of Schiff bases mainly due to the reduction and oxidation processes at the azomethine linkage. In most of the cases, the relation between peak current and square root of scan rate was studied. The studies revealed that the electrode processes are diffusion controlled. The ratio of the peak currents and peak separation values established that the most of the electrode process were quasi-reversible and

involves one electron transfer. CV recorded at a scan rate of 0.1 V/s with 5 scan cycles were appeared in the same position in all the cycles, suggesting that there is no adsorption of the compound on the glassy carbon electrode surface.

REFERENCES

- 1) P. T. Kissinger, W. R. Heineman, *J. Chem. Educ.*, 60, **1983**, 702
- 2) A. Pui, I. Berdan, I. M. Badarau, A. Gref and M. P. Fauvet, *Inorg. Chim. Acta.*, 320, **2001**, 167
- 3) F. Azevedo, C. Freire and B. D. Castro, *Polyhedron.*, 21, **2002**, 1695
- 4) R. Klement, F. Stock, H. Elias, H. Paulus, P. Pelikan, M. Valko and M. Mazur, *Polyhedron.*, 18, **1999**, 3617
- 5) P. G. Zhen Jia, W. B. Li, Y. M. Li and X. L. Zhang, *Asian. J. Chem.*, 20, **2008**, 1692
- 6) I. C. Santos, M. Vilas. Boas, M. F. M. Piedade, C. Freire, M. T. Duarte and B. De. Castro, *Polyhedron.*, 19, **2000**, 655
- 7) R. Ojani, J. B. Raouf and A. Alinezhad, *Electroanalysis.*, 14, **2002**, 1197
- 8) M. H. Pournaghi-Azar and R. Ojani, *Electrochim. Acta*, 39, **1994**, 953
- 9) R. N. Hegde, B. E. Kumara Swamy, B. S. Sherigara and S. T. Nandibewoor, *Int. J. Electrochem. Sci.*, 3, **2008**, 302
- 10) E. Niranjana, R. Raghavandra, Naik, B. E. Kumara Swamy, Y. D. Bodke, B. S. Sherigara, H. Jaradevappa, B. V. Badami, *Int. J. Electrochem. Sci.*, 3, **2008**, 980
- 11) N. P. Shetti, L. V. Sampangi, R. N. Hegde and S. T. Nandibewoor, *Int. J. Electrochem. Sci.*, 4, **2009**, 104
- 12) A. Habib, T. Shireen, A. Islam, N. Begum, A.M. S. Alam, *Pak. J. Anal. & Envir. Chem.*, 7 (2), **2006**, 96
- 13) N. Raman, S. Ravichandran, C. Thangaraja, *J. Chem. Sci.*, 116 (4), **2004**, 215

- 14) A. J. Zare , P. Ataeinia, *Life Science Journal*, 9(4), **2012**, 2396
- 15) A. D. Kulkarni, S. A. Patil, P. S. Badami, *Int. J. Electrochem. Sci.*, 4, **2009**, 717
- 16) S. Ershad, L. Sagathforoush, G. Karim-nezhad, S. Kangari, *Int. J. Electrochem. Sci.*, 4, **2009**, 846
- 17) A. Ourari, M. Khelafi, D. Aggoun, G. Bouet, M. A. Khan, *Adv. Phy. Chem.*, **2011**, doi:10.1155/2011/157484
- 18) A. J. Pearl and T. F. A. F. Reji, *J. Chem. Pharm. Res.*, 5(1), **2013**, 115
- 19) K. Y. Sharma, M. Prasad, *Orient. J. Chem.*, 28 (3), **2012**, 1419
- 20) L. A. Saghatforoush, B. Shabani, R. Khalilnezhad, M. Hasanzadeh, G. Karimnezhad, S. Ghammamy, *Asian J. Chem.*, 21(8), **2009**, 6317
- 21) S. Zolezzi, E. Spodine, A. Decinti, *Polyhedron.*, 21, **2002**, 55
- 22) F. A. Villamena, V. Horak, D. R. Crist, *Inorg. Chim. Acta.*, 342, **2003**, 125
- 23) S. Chandra, L. K. Gupta, Sangeetika, *Spectrochim. Acta., Part A: Molecular and Biomolecular Spectroscopy*, 62 (1–3), **2005**, 453
- 24) X. Lu, K. Zhu, M. Zhang, H. Liu, J. Kang. *J. Biochem. Biophys. Method.*, 52(3), **2002**, 189
- 25) Y. N. Zeng, N. Zheng, P.G. Osborne, Y. Z. Li, W.B. Chang, M. J. Wen, *J. Mol. Recogn.*, 15(4), **2002**, 204
- 26) M. Najafi, M. Rahbar, M. A. Naseri, *J. Electroanal. Chem.*, 655(2), **2011**, 111
- 27) J. M. Fernández-G, F. A. López-Durán, S. Hernández-Ortega, V. Gómez-Vidales, N. Macías-Ruvalcaba, M. Aguilar-Martínez, *J. Mol. Struct.*, 612(1), **2002**, 69

- 28) M. M. Ghoneim, E. M. Mabrouk, A. M. Hassanein, M. A. El-Attar, E. A. Hesham, *Central Eur. J. Chem.*, 5(3), **2007**, 898
- 29) J. Costamagna, L. E. Lillo, B. Matsuhira, M.D. Nosedá, M. Villagrán, *Carbohydr. Res.*, 338 (15), **2003**, 1535
- 30) S. Çakır, M. Odabas, E. Biçer, Z. Yazar, *J. Mol. Struct.*, 918, **2009**, 81
- 31) M. A. Neelakantan, F. Rusalraj, J. Dharmaraja, S. Johnsonraja, T. Jeyakumar, M. S. Pillai, *Spectrochim. Acta. A Mol. Biomol. Spectrosc.*, 71(4) **2008**, 1599 doi: 10.1016/j.saa.2008.06.008.
- 32) P. Muthuselvan, D. S. Theodore, N. M. Sivasankaran, *Asian J. Res. Chem.*, 4(8), **2011**, 1305
- 33) R.S. Nicholson, I. Shain, *Anal. Chem.*, 36, **1964**, 706
- 34) A.A. Isse, A. Gennaro, E. Vianello, *Electrochim. Acta*, 42, **1997**, 2065
- 35) T. Shono, N. Kise, E. Shirakawa, H. Matsumoto, E. Okazaki, *J. Org. Chem.*, 56, **1991**, 3063
- 36) N. Kise, H. Oike, E. Okazaki, M. Yoshimoto, T. Shono, *J. Org. Chem.*, 60, **1995**, 3980
- 37) A.J. Bard, L.R. Faulkner, *Electrochemical methods : Fundamentals and Applications*, John Wiley & Sons: New York, **1980**, 213
- 38) F. Gokmese, E. Gokmese, A.O. Solak, M. Isiklan, Z. Kihc, *J. Electroanal. Chem.*, 581, **2005**, 46
- 39) J.A. Harrison, Z.A. Khan, *J. Electroanal. Chem.*, 28, **1970**, 131